Desalination and Water Treatment
www.deswater.com

doi: 10.5004/dwt.2017.20962

82 (2017) 179–187
July

Removal of Pb(II) and Cu(II) from aqueous solutions by ultraviolet irradiation-modified biochar

Qiao Li[a,*], Yutao Gao[b], Jian Lang[a], Wenchuan Ding[c], Yi Yong[b]

[a]*PowerChina Chengdu Engineering Corporation Limited, Chengdu, 610072, China, Tel. +86-028-6571-2414, Fax +86-028-8278-9179, email: chidilq@163.com (Q. Li), Tel. +86-028-6779-2557, email: 2003001@chidi.com (J. Lang)*
[b]*Sichuan Academy of Environmental Sciences, Chengdu, 610041, China, Tel. +86-028-8544-2969, email: gyt0324@163.com (Y. Gao), Tel. +86-028-8510-9856, email: yongyi63@163.com (Y. Yong)*
[c]*National Centre for International Research of Low-carbon and Green Buildings, Chongqing University, Chongqing, 400045, China, Tel. +86-023-6543-3166, email: wcdz433@163.com (W. Ding)*

Received 1 September 2016; Accepted 19 May 2017

ABSTRACT

We herein report the modification of coconut shell-based biochar by ultraviolet (UV) irradiation to yield a highly efficient adsorbent for Pb(II) and Cu(II). Analysis of the physicochemical properties and structural characteristics of the modified biochar indicated that it contained a greater number of oxygen-containing functional groups on its surface compared with pristine biochar. In addition, the kinetics and adsorption isotherms for the adsorption of heavy metals by the biochar sample were investigated. More specifically, the pseudo-second order equation provided the best correlation for the adsorption process, and the adsorption isotherms fitted well with the Langmuir model. Furthermore, the Langmuir adsorption capacities of the modified biochar towards Pb(II) and Cu(II) were 66.86 and 7.78 mg g^{-1}, respectively, which represented 3.57- and 2.39-fold increases compared to the pristine biochar capacities. Moreover, batch sorption experiments demonstrated that the dosage and solution pH affected the removal of these metals from aqueous solutions by biochar. We also found that the adsorption mechanisms of Pb(II) and Cu(II) on modified biochar occurred mainly through surface sorption, likely involving the oxygen-containing functional groups present on the modified surface. Thus, we successfully demonstrated that UV irradiation is a promising modification approach for enhancing the adsorption ability of biochar.

Keywords: Biochar; Ultraviolet irradiation; Pb(II); Cu(II); Adsorption

1. Introduction

Biochar, a pyrogenic carbon-rich material produced from the pyrolysis of low-cost biomass in oxygen-limited conditions, has attracted much attention due to its potential applications in pollution control [1]. For example, the use of biochar in soil remediation has been reported [2,3], while recent studies have demonstrated that biochar can also act as an environmental adsorbent for many heavy metals, such as lead and copper, in wastewater [4,5]. However, the effectiveness of biochar as a heavy metal adsorbent varies greatly among different biochars, with modified biochars tending to exhibit significantly higher heavy metal sorption capacities than pristine biochar. As such, to enhance its adsorption capacity, extensive attention has recently been focused on the modification of biochar surface properties [6].

To date, various modification techniques have been employed to improve the functional group content and the surface area of biochar, including acidic and alkaline treatment methods, chemical oxidation, and chemical grafting [7–9]. However, the application of such methods resulted in secondary pollution due to the waste and surplus chemicals produced. As such, the development of an environmental friendly approach to biochar surface modification is of particular importance. For example, photochemical functionalization has been reported to induce functional group formation (e.g., carboxyl groups) on polymer and carbon

*Corresponding author.

surfaces [10–12], which indicates that the introduction of carboxylic groups onto the biochar surface may be possible through ultraviolet (UV) grafting without the generation of pollutants. However, to the best of our knowledge, the sorption ability of UV-modified biochar towards heavy metals has received little attention.

Ultraviolet irradiation can be divided into four main categories based on the wavelength of the irradiation, i.e., UV-A (315–380 nm), UV-B (280–315 nm), UV-C (200–280 nm), and UV-D (100–200 nm). Although UV grafting using UV-B irradiation at 254 nm has received the most attention, recent studies have shown that UV-A irradiation at 365 nm could also generate new polar groups (i.e., carboxyl groups) on the surfaces of polymer materials [13]. In addition, it has been proposed that the mechanism of UV grafting could involve free radical polymerization by UV irradiation. Furthermore, it should also be considered that a 365 nm UV light source is generated using a high-pressure mercury lamp, while a 254 nm UV light source is generated using low-pressure mercury lamp. As the high-pressure mercury lamp has a significantly stronger power and longer life, its use in industrial applications would be preferred.

Thus, we herein report the development of a simple and innovative method for the modification of biochar using UV-A irradiation at 365 nm, with the aim of significantly improving adsorptive performances towards heavy metals. For the purpose of this study we will examine the adsorption of lead (Pb(II)) and copper (Cu(II)), which are toxic and nonbiodegradable, and so pose a threat to human health [14]. In addition, the physicochemical properties of the biochar will be characterized and a range of experiments will be conducted to evaluate the sorption ability of the modified biochar. As such, our primary objectives are to compare the physicochemical properties of the pristine and modified biochars, to assess the adsorption ability of these materials towards Pb(II) and Cu(II), and to discuss the interaction mechanism between Pb(II), Cu(II), and the surface functional groups of the modified biochars.

2. Materials and methods

2.1. Materials

All chemicals and reagents employed through this study were of analytical grade. Aqueous solutions were prepared using deionized water (18.3 MΩ·cm, Barnstead UltraPure water). Lead nitrate ($Pb(NO_3)_2$), copper nitrate trihydrate ($Cu(NO_3)_2{\cdot}3H_2O$), sodium nitrate ($NaNO_3$), sodium hydroxide (NaOH), and nitric acid (HNO_3) were purchased from Chengdu Chemical Co. Ltd. Coconut shell residuals (the biomass feedstock) with particle sizes of 2–4 mm were collected in Hainan province, China.

2.2. Biochar production

Prior to pyrolysis, the biomass feedstock (500 g) was immersed in deionized water (1000 mL) for 2 h to remove all traces of dust. The washed biomass was then dried overnight at 100°C, after which, the samples were pyrolyzed in a tubular furnace (model SGMT100, Luoyang, China) at 700 ± 5°C for 2 h under a nitrogen atmosphere following heating at a rate of 10 ± 1°C min^{-1}. The resulting material was then allowed to cooled overnight prior to grinding to a particle size of 0.42–0.71 mm. The pristine biochar specimen will be referred to as BC for the remainder of this report.

2.3. Biochar modification

The above BC sample was spread out on a glass dish (Φ 150 mm) to give a sample thickness of ≤2 mm. The glass dish was then placed on a temperature-controlled heating panel beneath a UV lamp (high-pressure mercury lamp, 250 power, 365 nm emission line) positioned 10 cm from the sample. During the irradiation time of 16 h, the biochar samples were heated at 100°C. The modified biochars will herein be referred to as MBC.

2.4. Biochar characterization

The carbon, hydrogen, oxygen, and nitrogen contents of the biochar samples were analyzed using an elemental analyzer (model varioMACRO cube, ELEMENTAR Analysensysteme GmbH, Germany), while the surface functional group contents were determined by Boehm titrations [15]. In addition, Fourier transform infrared spectroscopy (FTIR) was carried out using an FTIR-8000 series spectrophotometer (model IRAffinity-1, SHIMADZU CORPORATION, Japan) between 4000 and 400 cm^{-1} with a resolution of 4.0 cm^{-1}. Furthermore, the pore structure parameters were determined using a specific surface area and porosity analyzer (model BELSORP-max, BEL JAPAN, INC).

2.5. Sorption experiments

The adsorption kinetics experiments were performed in 50 mL centrifuge tubes at 25 ± 0.5°C by mixing the biochar sample (30 mg) with solutions containing Pb(II) or Cu(II) (25 mL), which were prepared by dissolving their respective nitrate salts in a 0.01 mol L^{-1} $NaNO_3$ solution as the background electrolyte. The initial concentrations of Pb(II) and Cu(II) were 100 and 45 mg L^{-1}, respectively, and the initial pH values of the solutions were adjusted to pH 4.5 using 0.1 mol L^{-1} solutions of NaOH and HNO_3, as required. All bottles were then sealed and shaken at 100 rpm in a constant temperature water bath shaker (SHA-B, Lichen Corporation, China). Bottles were then withdrawn at a range of time intervals (i.e., 0, 0.5, 1, 2, 4, 8, 12, 24, and 48 h), and the samples were filtered immediately through nylon membrane filters (pore size = 0.22 μm). The Pb(II) and Cu(II) concentrations in the filtrates were determined by atomic absorption spectroscopy (AAS, WFX-210, Beifen-Ruili, China). The quantities of Pb(II) and Cu(II) adsorbed onto the biochar samples were calculated based on the differences between the initial and final concentrations of the metal species in the aqueous solutions.

For each adsorption isotherm experiment, a sample of the adsorbent (30 mg) was mixed with a solution containing the desired heavy metal (25 mL, 2–300 mg L^{-1}) in a centrifuge tube at 25 ± 0.5°C. The bottles were then shaken in a mechanical shaker at 25 ± 0.5°C for 48 h, after which time, the samples were withdrawn and immediately filtered to determine the Pb(II) and Cu(II) concentrations in the filtrate by AAS. The

residues were subsequently rinsed with deionized water, and dried at 60°C for use in further characterization tests.

The kinetic and isotherm experiments were performed in duplicate and the average values are reported. Additional analyses were conducted whenever two measurements showed a difference of >5%.

2.6. Effects of sorbent dosage and pH

To determine the effect of pH and sorbent dosage on the adsorption of the heavy metals by biochar, initial Pb(II) and Cu(II) concentrations of 5.0 and 0.1 mg L^{-1} were employed, respectively, and the temperature was maintained at 25 ± 0.5°C. Under these conditions, ~100% of the expected lead nitrate and copper nitrate trihydrate contents were present in the pH range 1.0–7.0, where the speciation distribution was obtained using the solubility product constants of lead and copper. To adjust the pH values of the heavy metal solutions, 0.1 mol L^{-1} solutions of NaOH and HNO_3 were employed as necessary.

The effect of adsorbent dosage on Pb(II) and Cu(II) adsorption was analyzed by the addition of various quantities of biochar (i.e., to give concentrations of 10, 20, 50, 100, and 200 mg L^{-1}) to 250 mL digestion vessels containing 100 mL of the Pb(II) and Cu(II) solutions (5.0 and 0.1 mg L^{-1}, respectively). The effect of pH on the adsorption of the Pb(II) and Cu(II) were determined by varying the solution pH (i.e., pH 2–7) and using adsorbent (biochar) dosages of 100 and 10 mg L^{-1}, respectively. After shaking the samples for 48 h in a mechanical shaker at 25 ± 0.5°C, the quantities of heavy metal ions adsorbed were determined using the procedures described above.

3. Results and discussion

3.1. Biochar properties

To investigate the properties of the biochar samples, we first used N_2 adsorption-desorption isotherms to analyze the structural characteristics of these materials. Fig. 1 shows the adsorption-desorption isotherms belong to type I, which displays the existence of abundant microporous structures in the biochars.

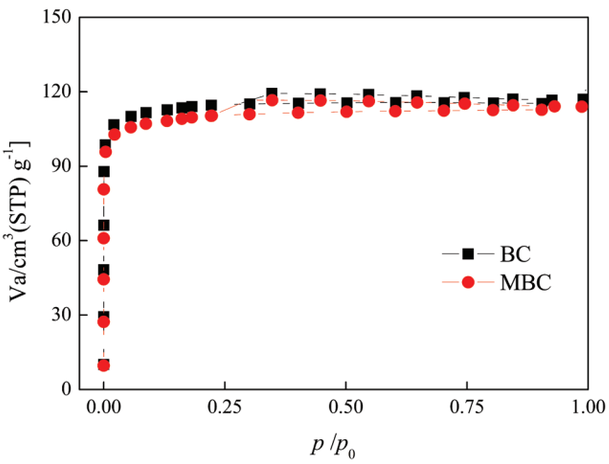

Fig. 1. N_2 adsorption-desorption isotherms of the pristine (BC) and modified (MBC) at 77K.

The pore structure parameters of the biochar samples were calculated from the isotherms outlined in Table 1 using BEL Japan software. In addition, the Brunauer-Emmett-Teller (BET) surface areas (a_s) and average pore sizes (r_p) were calculated using the BET method [16], while the micropore volumes (V_1) were calculated using the MP-plot method [17], and the mesoporous volumes (V_2) were calculated using the Barrett-Joyner-Halenda (BJH) method [18]. Furthermore, the pore surface areas (a_1) and the external surface areas (a_2) were calculated using the *t*-plot method [19].

As shown in Table 1, UV irradiation substantially enhanced the external surface area of the biochar samples, with the MBC external surface area increasing 3.63-fold compared to that of the pristine BC sample, while the pore surface area changed in reverse order, thus predicating that MBC suffered from pore collapse in modification process. Moreover, this pore-collapse reaction also could be confirmed by the other parameters investigation, including the BET surface area, the micropore volume, the mesopore volume, and the average pore radius. However, these results showed that the textural structure of biochar was not signally altered following UV irradiation.

In contrast, the results obtained from Boehm titrations (Table 2) indicated a significant increase in the number of acidic groups present on the biochar surface following UV irradiation. For example, the carboxyl group content increased 5.1-fold on MBC compared to that of BC, while the total number of acidic groups increased 3.75-fold. In addition, a significant increase in the number of lactonic and phenolic groups was also observed. This is of particular interest, after used for Pb(II) and Cu(II) adsorption, the oxygen-containing functional groups on both BC and MBC had a sharp decrease, therefore suggesting that the Pb(II) and Cu(II) adsorption process on biochar may be controlled by the oxygen-containing functional groups. Furthermore, as previous studies have demonstrated that the presence of oxygen-containing functional groups can enhance heavy metal sorption through surface electrostatic attractions and/or surface complexation [20,21].

3.2. Adsorption kinetics

We then moved on to examine the adsorption kinetics of the BC and MBC samples. As shown in Fig. 2, rapid sorp-

Table 1
Physicochemical properties of the pristine (BC) and modified (MBC) biochars

	BC	MBC
a_s (m^2 g^{-1})	450.96	433.06
a_1 (m^2 g^{-1})	472.61	453.54
a_2 (m^2 g^{-1})	0.90	3.27
V_1 (cm^3 g^{-1})	0.19	0.18
V_2 (cm^3 g^{-1})	0.01	0.02
r_p (nm)	1.61	1.65

Table 2
Results of Boehm titration of the fresh and used biochars

Parameter	BC			MBC		
	Fresh	Used for Pb(II)	Used for Cu(II)	Fresh	Used for Pb(II)	Used for Cu(II)
Carboxyl (mmol g^{-1})	0.15	0.02	0	0.76	0.07	0.02
Lactonic (mmol g^{-1})	0.09	0.06	0.01	0.16	0.03	0.03
Phenolic (mmol g^{-1})	0.04	0.01	0.01	0.13	0.02	0.03
Total of acidic groups (mmol g^{-1})	0.28	0.09	0.02	1.05	0.12	0.08
Basic groups (mmol g^{-1})	0.38	0.31	0.32	0.37	0.35	0.33

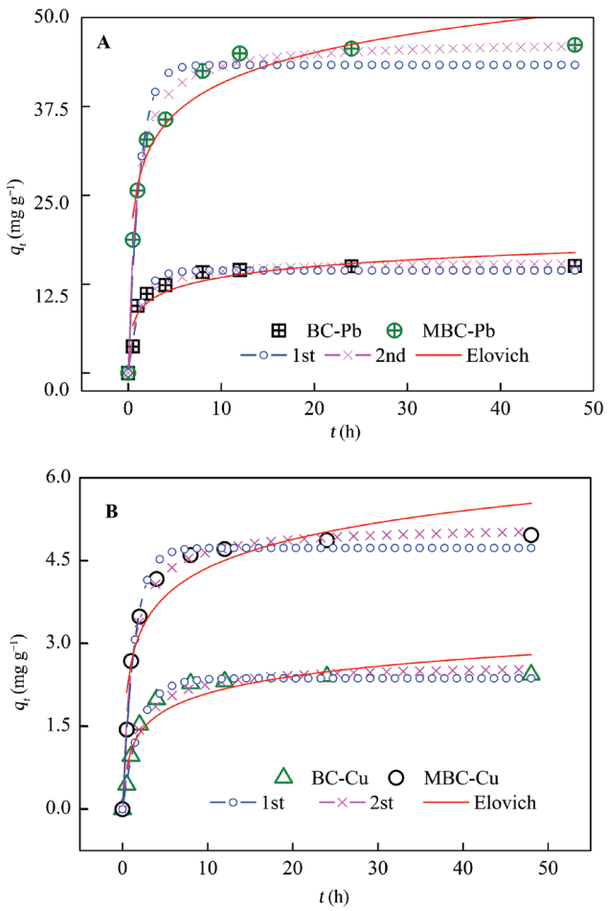

Fig. 2. Sorption kinetics data and fitted models of heavy metals onto the pristine (BC) and modified (MBC) biochars: (A) Pb(II) and (B) Cu(II) (Experimental conditions: [Pb(II)] = 100 mg L^{-1}, [Cu(II)] = 45 mg L^{-1}, pH = 4.5, and T = 25 ± 0.5°C.).

tion kinetics were observed for Pb(II) and Cu(II) on both BC and MBC in the initial phase, although this was followed by a slow sorption phase until saturation was reached. Indeed, these results are similar to those of previous studies [13,22]. More specifically, over the initial few hours, >60% sorption was observed for both Pb(II) and Cu(II), with the sorption performance of MBC being greater than that of BC.

Thus, to gain further insight into the sorption process, pseudo-first (Eq. (1)) and pseudo-second order equations [Eq. (2)] were employed in addition to the Elovich equation [Eq. (3)] [23–25].

$$\ln(qe - qt) = \ln qe - k_1 t \quad (1)$$

$$t / q_t = 1 / \left(k_2 q_e^2\right) + t / q_e \quad (2)$$

$$q_t = \frac{1}{b}\ln t + \frac{1}{b}\ln ab \quad (3)$$

where k_1 (h^{-1}) is the rate constant of first-order adsorption, k_2 (g mg^{-1} h^{-1}) is the rate constant of second-order adsorption, and a (mg g^{-1} h^{-1}) and b (g mg^{-1}) are constants. More specifically, a can be regarded as the initial adsorption rate. The kinetic parameters calculated using the above models are listed in Table 3.

As indicated, the sorption of Pb(II) and Cu(II) by the biochar samples corresponded well with the pseudo-second-order kinetic model, where R^2 > 0.97. These results correspond with previous studies describing the removal of heavy metals [26,27], therefore suggesting that the adsorption of Pb(II) and Cu(II) onto biochar may be controlled by the availability of biochar surface sites rather than by the concentration of heavy metal ions [28,29]. In addition, a few reports have suggested that Pb(II) and Cu(II) sorption onto biochar could involve surface complexation and/or surface precipitation [30].

The initial sorption rate (h) of the pseudo-second-order kinetic model can be calculated by Eq. (4) [31].

$$[t \to 0] \quad h = k_2 \times q_e^2 \quad (4)$$

Upon examination of the data outlined in Table 3, it was clear that the initial sorption rates (h) of MBC were greater than that of BC. More specifically, the initial sorption rates of Pb(II) and Cu(II) on MBC were approximately 3.28- and 3.09-fold greater than those on BC, respectively. Thus, based on the characterization results presented above, we expect that this difference is due to the increase in surface oxygen-containing functional groups.

3.3. Adsorption isotherms

We subsequently employed the Langmuir [Eq. (5)], Freundlich [Eq. (6)], and Temkin equations [Eq. (7)] for analysis

Table 3
The kinetic parameters of the pristine (BC) and modified (MBC) biochars for lead and copper

Models and parameters	Pb		Cu	
	BC	MBC	BC	MBC
Pseudo-first-order kinetic model				
q_e (mg g^{-1})	14.430	43.354	2.373	4.735
k_1 (h^{-1})	0.397	0.418	0.245	0.360
R^2	0.968	0.954	0.996	0.988
Pseudo-second-order kinetic model				
q_e (mg g^{-1})	15.636	46.751	2.616	5.130
k_2 (g mg^{-1} h^{-1})	0.018	0.006	0.061	0.049
R^2	0.974	0.993	0.998	0.995
h (g mg^{-1} h^{-1})	4.001	13.114	0.417	1.290
Elovich equation				
a (mg g^{-1} h^{-1})	93.123	426.905	4.907	26.418
b (g.mg^{-1})	0.112	0.040	0.560	0.336
R^2	0.908	0.967	0.923	0.936

of the adsorption isotherms, as these classic empirical models for examining the adsorption isotherms of ions express the relationship between the adsorbate and the sorbent surface properties and affinity [32–34].

$$q_e = \frac{q_m \cdot k_L \cdot C_e}{(1 + k_L \cdot C_e)} \quad (5)$$

$$q_e = K_f \cdot C_e^{1/n} \quad (6)$$

$$q_e = B\ln A + B\ln Ce \quad (7)$$

q_e is the quantity of heavy metal sorption onto the adsorbent at equilibrium (mg g^{-1}), C_e is the equilibrium concentration (mg L^{-1}), k_L represents the Langmuir bonding term related to the interaction energy (L mg^{-1}), q_m denotes the Langmuir maximum capacity (mg g^{-1}), A and B are constants related to the adsorption capacity and the intensity of adsorption, respectively, K_f represents the equilibrium constant parameters ((mg g^{-1}) (mg L^{-1})$^{-1/n}$), and $1/n$ correlates the effect of concentration to the degree of adsorption (where n >1, sorption is favorable).

These models were further validated by root-mean-square deviation (RSMD) [35], as shown in Table 4.

$$RSMD = \left[1/n\sum\left(q_{\exp} - q_p\right)^2\right]^{1/2} \quad (8)$$

where n is the number of data points, and q_{exp} (mg g^{-1}) and q_p (mg g^{-1}) are the experimental and calculated adsorption capacities, respectively. In this case, lower RMSD values are preferable, as they suggest optimal estimated model performance.

The adsorption isotherms of both Pb(II) and Cu(II) on the BC and MBC samples exhibited typical "L" shapes (Fig. 3).

Table.4
The adsorption isotherm parameters of lead and copper on the pristine biochar (BC) and modified biochar (MBC)

Models and Parameters	BC		MBC	
	Pb	Cu	Pb	Cu
Langmuir model				
q_m (mg g^{-1})	18.719	3.253	66.860	7.784
k_L (L mg^{-1})	0.066	0.064	0.078	0.090
R^2	0.988	0.995	0.991	0.996
RSMD	0.443	0.070	2.160	0.136
Freundlich isotherm				
K_f (mg g^{-1}) (mg L^{-1}) $^{-1/n}$	5.817	0.992	21.125	2.800
n	4.802	4.775	4.756	5.429
R^2	0.904	0.954	0.953	0.970
RSMD	1.346	0.199	5.559	0.387
Temkin equation				
A (L mg^{-1})	1.384	1.576	1.937	3.550
B	3.150	0.527	10.814	1.136
R^2	0.941	0.972	0.973	0.983
RSMD	0.908	0.154	3.307	0.294

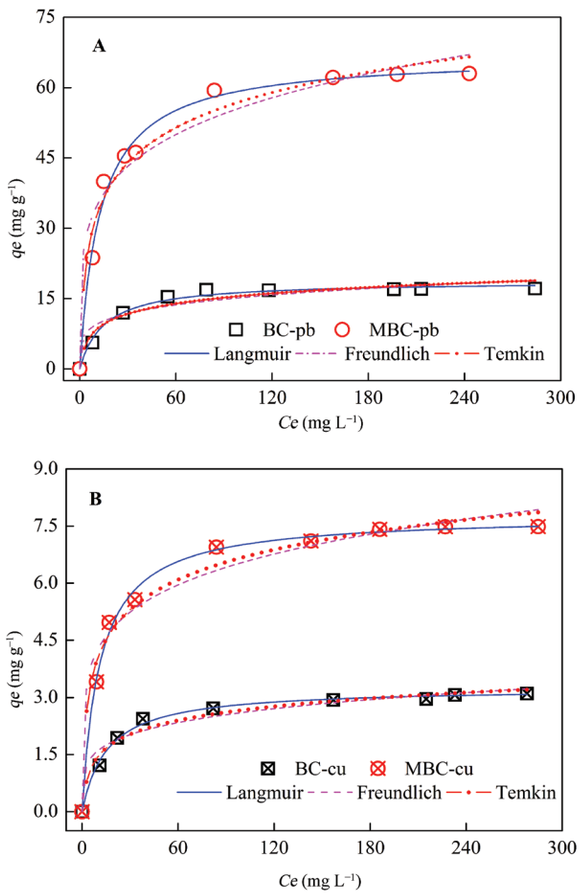

Fig. 3. Sorption isotherm data and fitted models of heavy metals onto the pristine (BC) and modified (MBC) biochars: (A) Pb(II) and (B) Cu(II) (Experimental conditions: pH = 4.5, T = 25 ± 0.5°C.).

The various parameters and regression data for the sorption of Pb(II) and Cu(II) onto the biochar samples at 25 ± 0.5°C are shown in Table 4. Interestingly, the obtained correlation coefficients suggested that the Langmuir model was a better fit for the adsorption isotherms of both heavy metals than the Freundlich and Temkin models ($R^2 > 0.988$ for the Langmuir model versus 0.904–0.970 and 0.941–0.983 for the Freundlich and Temkin models, respectively). Furthermore, the RSMD decreased in the following order: Freundlich > Temkin > Langmuir, thus confirming that the Langmuir model provided the best fit. These results indicate a homogeneous distribution of active sites on the biochar surface in addition to a monolayer adsorption process [36,37].

The essential characteristics of the Langmuir isotherm can be expressed by a dimensionless constant known as the equilibrium parameter R_L [38]:

$$R_L = \frac{1}{1 + k_L \rho_e} \tag{9}$$

where the value of R_L indicates whether the isotherm is unfavorable ($R_L > 1$), linear ($R_L = 1$), favorable ($0 < R_L < 1$), or irreversible ($R_L = 0$). As the R_L values of our system ranged between 0 and 1, we could therefore conclude that the adsorption of Pb(II) and Cu(II) onto biochar was favorable.

According to the Langmuir model, the maximum adsorption capacities of Pb(II) and Cu(II) on MBC at 25 ± 0.5°C (i.e., 66.86 and 7.78 mg g^{-1}) were significantly higher than those on BC (i.e., 18.72 and 3.25 mg g^{-1}). In addition, the adsorption capacities of Pb(II) and Cu(II) were enhanced 3.57- and 2.39-fold on MBC, respectively.

The affinities of the binding sites to metal ion sorption onto biochar were then evaluated by examination of the k_L values. More specifically, the k_L values for MBC (0.078 and 0.090 L mg^{-1}, for Pb(II) and Cu(II), respectively) were greater than those for BC (0.066 and 0.064 L mg^{-1}, respectively), indicating the stronger affinity of MBC towards these heavy metal ions. We therefore expected that this enhanced affinity was due to the presence of additional oxygen-containing functional groups on the MBC surface.

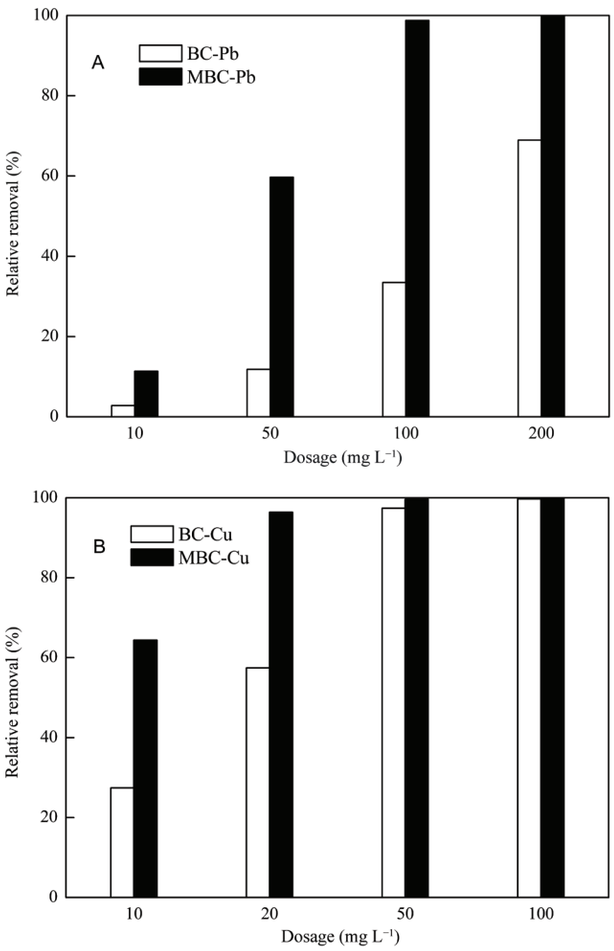

Fig. 4. Effects of sorbent dosage on heavy metal adsorption onto the pristine (BC) and modified (MBC) biochars: (A) Pb(II) and (B) Cu(II) (Experimental conditions: [Pb(II)] = 5 mg L^{-1}, [Cu(II)] = 0.1 mg L^{-1}, pH = 5, and T = 25 ± 0.5°C.).

3.4. Effects of sorbent dosage and solution pH

As shown in Fig. 4, the rates of Pb(II) and Cu(II) removal increased upon increasing the biochar dosage. For an initial Pb(II) concentration of 5 mg L^{-1}, the removal rate increased from 11.3% to 98.7% when the MBC dosage was increased from 10 to 100 mg L^{-1}, with a further gradual increase being observed up to an MBC dosage of 200 mg L^{-1}. Similarly, for an initial Cu(II) concentration of 0.1 mg L^{-1}, the removal rate increased from 64.4% to 96.4% upon increasing the MBC dosage from 10 to 20 mg L^{-1}. A similar trend was observed for the adsorption on BC. These results therefore indicated that the optimal MBC dosages for the removal of Pb(II) (5 mg L^{-1}) and Cu(II) (0.1 mg L^{-1}) were 100 and 20 mg L^{-1}, respectively.

The effect of the initial solution pH on Pb(II) and Cu(II) sorption was then examined. As shown in Fig. 5, significant variations in heavy metal sorption onto the MBC and pristine BC samples were observed upon varying the solution pH, with the degree of sorption increasing gradually with increasing pH between pH 2 and 7. Indeed, these results are consistent with a number of previous studies [39–41]. This variation in sorption with pH could be accounted for by the H^+ ions in solution competing with Pb(II) and Cu(II) for the biochar binding sites at low pH values, in addition to the majority of oxygen-containing functional groups on the biochar surfaces being protonated to yield either positively charged or neutral surfaces. In contrast, at high pH values, the H^+ concentration was reduced, thus leading to increased heavy metal sorption onto the biochar.

3.5 Adsorption mechanisms

As previously discussed in the context of Boehm titrations, the abundance of oxygen-containing functional groups on the biochar surface increased following UV irradiation. Indeed, this was confirmed by FTIR analysis (Fig. 6), where signals corresponding to the carboxylic C=O (MBC) and aromatic C=C (BC and MBC) stretching vibrations were observed at 1700–1740 cm^{-1} and 1630–1680 cm^{-1}, respectively [42].

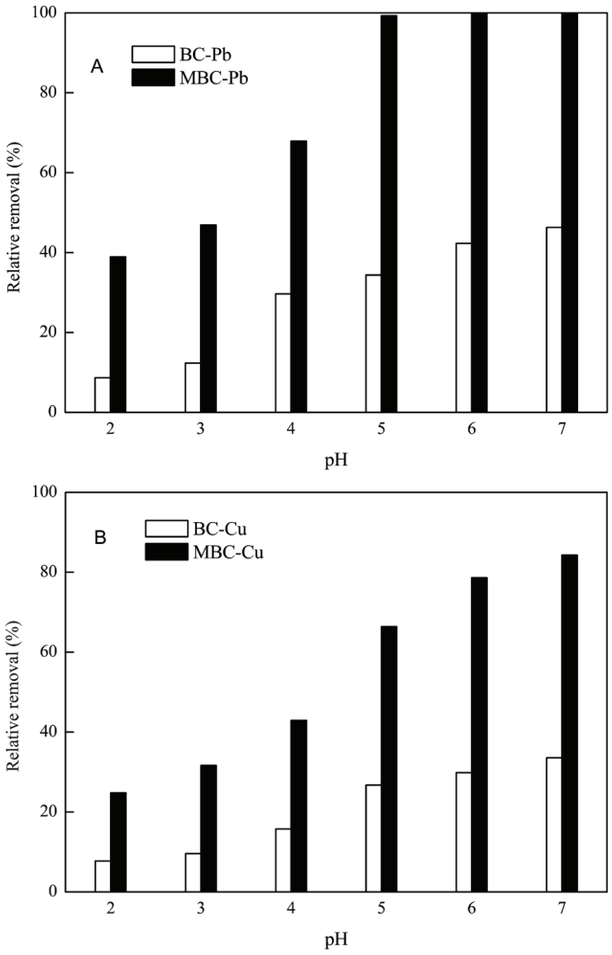

Fig. 5. Effects of solutions pH on heavy metal adsorption onto the pristine (BC) and modified (MBC) biochars: (A) Pb(II) and (B) Cu(II) (Experimental conditions: [Pb(II)] = 5 mg L^{-1}, [Cu(II)] = 0.1 mg L^{-1}, and $T = 25 \pm 0.5^{o}$C.).

Interestingly, following Pb/Cu sorption, the intensity of the signals at 1740 and 1630 cm^{-1} decreased in the MBC samples, while those between 1700–1740 cm^{-1} essentially disappeared. Similarly, the intensities of the C=C stretching vibrations of BC at 1630 cm^{-1} also decreased following Pb/Cu sorption. These observations indicated that the adsorption of Pb(II) and Cu(II) sorption by BC and MBC likely occurred via a surface sorption mechanism through the coordination of Pb(II) and Cu(II) d electrons to the C=C bond. In the case of the MBC sample, adsorption was enhanced through the presence of additional O–Pb and O–Cu surface interactions, which corresponds with the observations of previous reports [43]. Considering that biochar had high stability in moist conditions and its molecular structure was characterized by rings of six C atoms linked together [44,45], the possible adsorption mechanisms for the two biochar samples can be described schematically as following equations [Eqs. (10)–(13)]. Moreover, this interactions between biochar and metal ions maybe increase its stability [46].

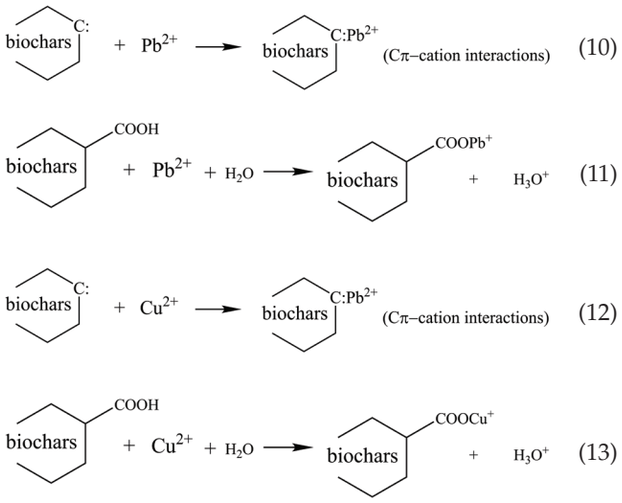

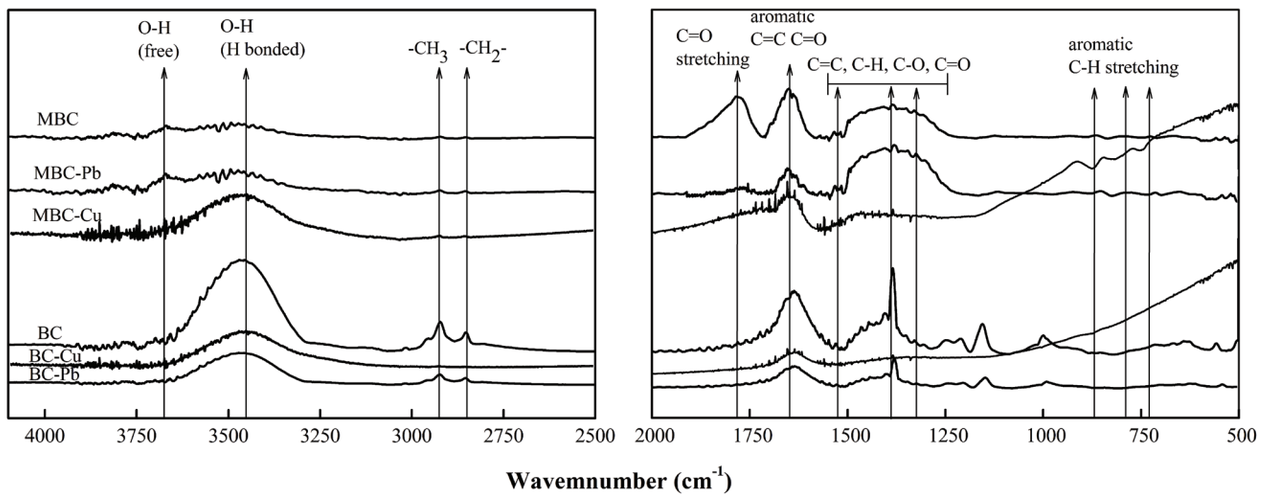

Fig. 6. The FTIR of the pristine (BC) and modified (MBC) biochars before and after reaction with aqueous Pb(II) and Cu(II).

4. Conclusions

We herein reported the use of an ultraviolet (UV) irradiation method for the modification of coconut shell-based biochar (BC) to increase the efficiency of BC in the adsorption of the heavy metal Pb(II) and Cu(II) ions from aqueous solutions. Following examination of the physicochemical properties and structural characteristics of the modified biochar (MBC) sample, we confirmed that the quantity of oxygen-containing functional groups on the external MBC surface area had increased significantly, thus enhancing the removal of Pb(II) and Cu(II) compared to the pristine BC sample. Furthermore, evaluation of the kinetics and adsorption isotherms for the adsorption process indicated that Pb(II) and Cu(II) sorption by biochar likely occurred via a surface sorption mechanism, where the Langmuir isotherm model and pseudo-second order kinetics appeared to dominate. We also observed that increased sorbent dosages and higher pH values enhanced heavy metal adsorption by both BC and MBC. We could therefore conclude that the reported UV modification method is suitable for the preparation of highly efficient biochars for heavy metal remediation.

Acknowledgments

This work was partially supported by Major Science and Technology Project of Water Pollution Control and Management in China (2012ZX07102-001-004). The authors are also grateful to the anonymous reviewers for their invaluable insight and helpful suggestions.

References

[1] X. Tan, Y. Liu, G. Zeng, W. Xin, X. Hu, Y. Gu, Z. Yang, Application of biochar for the removal of pollutants from aqueous solutions, Chemosphere, 125 (2015) 70–85.
[2] K. Lu, Y. Xing, G. Gielen, N. Bolan, S.O. Yong, N.K. Niazi, X. Song, G. Yuan, C. Xin, X. Zhang, Effect of bamboo and rice straw biochars on the mobility and redistribution of heavy metals (Cd, Cu, Pb and Zn) in contaminated soil, J. Environ. Manage., 186 (2017) 285–292.
[3] A.P. Puga, C.A. Abreu, L.C.A. Melo, L. Beesley, Biochar application to a contaminated soil reduces the availability and plant uptake of zinc, lead and cadmium, J. Environ. Manage., 159 (2015) 86–93.
[4] J. Meng, X. Feng, Z. Dai, X. Liu, J. Wu, J. Xu, Adsorption characteristics of Cu(II) from aqueous solution onto biochar derived from swine manure, Environ. Sci. Pollut. R., 21 (2014) 7035–7046.
[5] H. Wang, B. Gao, S. Wang, J. Fang, Y. Xue, Y. Kai, Removal of Pb(II), Cu(II), and Cd(II) from aqueous solutions by biochar derived from $KMnO_4$ treated hickory wood, Biores. Technol. 197 (2015) 356–362.
[6] G.X. Yang, H. Jiang, Amino modification of biochar for enhanced adsorption of copper ions from synthetic wastewater, Water Res., 48 (2014) 396–405.
[7] S. Wang, B. Gao, A.R. Zimmerman, Y. Li, L. Ma, W.G. Harris, K.W. Migliaccio, Removal of arsenic by magnetic biochar prepared from pinewood and natural hematite, Biores. Technol., 175 (2015) 391–395.
[8] A.S.K. Warahena, C. Yew Khoy, Energy recovery efficiency and cost analysis of VOC thermal oxidation pollution control technology, Environ. Sci. Technol., 43 (2009) 6101–6105.
[9] M. Ying, W.J. Liu, Z. Nan, Y.S. Li, J. Hong, G.P. Sheng, Polyethylenimine modified biochar adsorbent for hexavalent chromium removal from the aqueous solution, Biores. Technol., 169 (2014) 403–408.
[10] M.D. Ellison, L.K. Buckley, G.G. Lewis, C.E. Smith, E.M. Siedlecka, C.V. Palchak, J.M. Malarchik, Photochemical hydroboration-oxidation of single-walled carbon nanotubes, J. Phys. Chem. C., 113 (2009) 18536–18541.
[11] T. Nakamura, Photochemical modification and functionalization of carbon surfaces with fluorine moieties, Diam. Relat. Mater., 19 (2010) 374–381.
[12] T. Nakamura, T. Ohana, Photochemical modification of DLC films with oxygen functionalities and their chemical structure control, Diam. Relat. Mater., 33 (2013) 16–19.
[13] Y. Tsuda, M. Tahira, N. Shinohara, D. Sakata, Effect of photoacid generator on surface wettability controllable polyimides by UV light irradiation, J. Photopolym. Sci. Tec., 28 (2015) 313–318.
[14] R. Kumar, M. Rani, H. Gupta, B. Gupta, Trace metal fractionation in water and sediments of an urban river stretch, Chem. Spec. Bioavailab., 26 (2014) 200–209.
[15] H.P. Boehm, Surface oxides on carbon and their analysis: a critical assessment, Carbon, 40 (2002) 145–149.
[16] S. Brunauer, P.H. Emmett, E. Teller, Adsorption of gases in multimolecular layers, J. Am. Chem. Soc., 60 (1938) 309–319.
[17] R.S. Mikhail, S. Brunauer, E.E. Bodor, Investigations of a complete pore structure analysis: I. Analysis of micropores, J. Colloid. Interf. Sci., 26 (1968) 45.
[18] E.P. Barrett, L.G. Joyner, P.P. Halenda, The determination of pore volume and area distributions in porous substances. I. Computations from Nitrogen isotherms, J. Am. Chem. Soc., 73 (1951) 373.
[19] B.C. Lippens, J.H.D. Boer, Studies on pore systems in catalysts V. The *t* method, J. Catalysis, 4 (1965) 319–323.
[20] H. Jin, S. Capareda, Z. Chang, J. Gao, Y. Xu, J. Zhang, Biochar pyrolytically produced from municipal solid wastes for aqueous As(V) removal: Adsorption property and its improvement with KOH activation, Biores. Technol., 169 (2014) 622–629.
[21] Y. Xue, B. Gao, Y. Yao, M. Inyang, M. Zhang, A.R. Zimmerman, K.S. Ro, Hydrogen peroxide modification enhances the ability of biochar (hydrochar) produced from hydrothermal carbonization of peanut hull to remove aqueous heavy metals: Batch and column tests, Chem. Eng. J., 200–202 (2012) 673–680.
[22] D. Kołodyńska, R. Wnętrzak, J.J. Leahy, M.H.B. Hayes, W. Kwapiński, Z. Hubicki, Kinetic and adsorptive characterization of biochar in metal ions removal, Chem. Eng. J., 197 (2012) 295–305.
[23] Y. Zhou, B. Gao, A.R. Zimmerman, J. Fang, Y. Sun, X. Cao, Sorption of heavy metals on chitosan-modified biochars and its biological effects, Chem. Eng. J., 231 (2013) 512–518.
[24] Y.S. Ho, G. Mckay, Pseudo-second order model for sorption processes, Process Biochem., 34 (1999) 451–465.
[25] M.J.D. Low, Kinetics of chemisorption of gases on solids, Chem. Rev., 60 (1960) 267–312.
[26] P. Khare, U. Dilshad, P.K. Rout, V. Yadav, S. Jain, Plant refuses driven biochar: Application as metal adsorbent from acidic solutions, Arab. J .Chem., 269 (2013).
[27] Z. Liu, F.S. Zhang, Removal of lead from water using biochars prepared from hydrothermal liquefaction of biomass, J. Hazard. Mater., 167 (2009) 933–939.
[28] Y.S. Ho, G. Mckay, Pseudo-second order model for sorption processes, Process Biochem., 34 (1999) 451–465.
[29] Y. Liu, New insights into pseudo-second-order kinetic equation for adsorption, Colloids Surf. A Physicochem. Eng. Asp., 320 (2008) 275–278.
[30] P. Regmi, J.L.G. Moscoso, S. Kumar, X. Cao, J. Mao, G. Schafran, Removal of copper and cadmium from aqueous solution using switchgrass biochar produced via hydrothermal carbonization process, J. Environ. Manage., 109 (2012) 61–69.
[31] G. Güçlü, E. Al, S. Emik, T. B. İyim, S. Özgümüş, M. Özyürek, Removal of Cu^{2+} and Pb^{2+} ions from aqueous solutions by starch-graft-acrylic acid/montmorillonite superabsorbent nanocomposite hydrogels, Polym. Bull., 65 (2010) 333–346.

[32] I. Langmuir, The adsorption of gas on plane surfaces of glass, mica and platinum, J. Am. Chem. Soc., 143 (1918) 1361–1403.
[33] H.M.F. Freundlich, Uber die adsorption in losungen, Z. Phsy. Chem., 57 (1906) 385–470.
[34] C. Aharoni, M. Ungarish, Kinetics of activated chemisorption. Part 2. Theoretical models, J. Chem. Soc. Far. Trans., 73 (1977) 456–464.
[35] N.S. Nasri, U.D. Hamza, S.N. Ismail, M.M. Ahmed, R. Mohsin, Assessment of porous carbons derived from sustainable palm solid waste for carbon dioxide capture, J. Clean. Prod., 71 (2014) 148–157.
[36] X. Chen, G. Chen, L. Chen, Y. Chen, J. Lehmann, M.B. Mcbride, A.G. Hay, Adsorption of copper and zinc by biochars produced from pyrolysis of hardwood and corn straw in aqueous solution, Biores. Technol., 102 (2011) 8877–8884.
[37] X.J. Hu, J.S. Wang, Y.G. Liu, X. Li, G.M. Zeng, Z.L. Bao, X.X. Zeng, A.W. Chen, F. Long, Adsorption of chromium (VI) by ethylenediamine-modified cross-linked magnetic chitosan resin: Isotherms, kinetics and thermodynamics, J. Hazard. Mater., 185 (2010) 306–314.
[38] T.W. Weber, R.K. Chakravorti, Pore and solid diffusion models for fixed-bed adsorbers, Aiche J., 20 (1974) 228–238.
[39] X.J. Tong, J.Y. Li, J.H. Yuan, R.K. Xu, Adsorption of Cu(II) by biochars generated from three crop straws, Chem. Eng. J., 172 (2011) 828–834.
[40] M. Inyang, B. Gao, Y. Ying, Y. Xue, A.R. Zimmerman, P. Pullammanappallil, X. Cao, Removal of heavy metals from aqueous solution by biochars derived from anaerobically digested biomass, Biores. Technol., 110 (2012) 50–56.
[41] H. Lu, W. Zhang, Y. Yang, X. Huang, S. Wang, R. Qiu, Relative distribution of Pb^{2+} sorption mechanisms by sludge-derived biochar, Water Res., 46 (2011) 854–862.
[42] B. Chen, D. Zhou, L. Zhu, Transitional adsorption and partition of nonpolar and polar aromatic contaminants by biochars of pine needles with different pyrolytic temperatures, Environ. Sci. Technol., 42 (2008) 5137–5143.
[43] X. Dong, L.Q. Ma, Y. Li, Characteristics and mechanisms of hexavalent chromium removal by biochar from sugar beet tailing, J. Hazard. Mater., 190 (2011) 909–915.
[44] G.X. Yang, H. Jiang, Amino modification of biochar for enhanced adsorption of copper ions from synthetic wastewater, Water Res., 48 (2014) 396–405.
[45] O. Mašek, P. Brownsort, A. Cross, S. Sohi, Influence of production conditions on the yield and environmental stability of biochar, Fuel, 103 (2011) 151–155.
[46] C.H. Cheng, J. Lehmann, J.E. Thies, S.D. Burton, Stability of black carbon in soils across a climatic gradient, J. Geophys. Res., 113 (2008) 50–55.